JOURNAL OF MATERIALS SCIENCE 28 (1993) 2789–2794

Grain-growth in nanocrystalline zirconium-based alloys

T. SPASSOV*, U. KÖSTER
Department of Chemical Engineering, University of Dortmund D-4600 Dortmund 50, Germany

Crystallization and subsequent grain growth in nanocrystalline $Fe_{33}Zr_{67}$ and $(Fe,Co)_{33}Zr_{67}$ alloys were studied by TEM, differential scanning calorimetry and X-ray diffraction. The grain-growth data for both alloys obtained over a wide temperature range (about 200 °C) were fitted to different kinetic equations (with different grain-growth exponent, n). The model with $n = 3$ (Equations 4 and 5) was found to predict in the best way the isothermal experimental data. This result gives strong evidence that crystallization (in our case by a polymorphic reaction) is indeed observed of a glass into a nanocrystalline material prior to the coarsening, rather than grain growth in an extremely fine-grained material which was never glassy at all. The activation energies for grain-growth, $-260 \pm 25\ kJ\ mol^{-1}$, were found to be practically the same for both systems. Additional information about the crystal growth kinetics of the nanocrystals in the amorphous matrix was obtained for $(Fe,Co)_{33}Zr_{67}$ glass.

1. Introduction

Crystallization of zirconium-based intertransition metallic glasses has been intensively investigated by differential scanning calorimetry (DSC) [1–5], resistivity measurements [3, 4, 6], X-ray diffraction [3–5, 7, 8], and electron microscopy (TEM) [3, 8–10]. Most of these studies focused on crystallization kinetics, microstructure and crystalline phase sequence of binary zirconium-based metallic glasses aged under different thermal conditions. Coarsening of the metastable nanocrystalline fcc $FeZr_2$ crystals has been observed [3, 11] during crystallization of $Fe_{33}Zr_{67}$ amorphous alloy. Theoretical and experimental studies of grain-growth in single-phase systems [12], as well as in two-phase alloys [13] have been extensively carried out for many years. Reliable data, however, on grain growth in nanocrystalline materials and grain-growth kinetics are still not available.

The driving force for the grain-growth process is the decrease in interfacial free energy. Beck *et al.* [14] have proposed an equation for grain growth in which the rate of grain-size change is proportional to $\sigma/\bar{D}$, where σ is the grain-boundary interfacial energy and $\bar{D}$ is the mean grain size. Burke and Turnbull [15] deduced a parabolic relationship for grain-growth kinetics, which can be represented for isothermal annealing in the general form as

$$\bar{D}^2 - \bar{D}_0^2 = Kt \quad (1)$$

where $\bar{D}$ is the mean grain diameter (size) at time t, $\bar{D}_0$ is the mean initial grain size, and K is a constant. Assuming that $\bar{D} \gg \bar{D}_0$

$$\bar{D}^2 = Kt \quad (2)$$

It is known that except at temperatures near the melting point, Equation 1 is not satisfied and grain growth in metals is better described by the empirical equation

$$\bar{D} = K' t^{1/n} \quad (3)$$

where n is the grain-growth exponent which, in most of the experimental works, is about 3 ($n > 2$).

A variety of different values of n have been reported in the literature corresponding to various metallic systems (pure single phase as well in two-phase and those containing impurities). Generally, the values of n vary from 2–4 with a most frequently seen value of $n = 3$. Most of the investigators tried to explain the exponents in terms of the parabolic grain-growth kinetics ($n = 2$) or looked for ways to explain the deviation from the ideal case $n = 2$, making different assumptions for the connection between the conditions controlling the grain growth and the values of n. Attempts have been made, on the basis of the results on kinetics of grain growth and microstructural studies, to isolate certain mechanisms of grain growth and to connect them with certain values of n. So far, a general theory of grain growth, explaining the variety of different n values experimentally obtained, does not exist.

The activation energy for grain-growth can be reliably determined from studies of the mean grain diameter (if the constant K in Equations 1–3 depends exponentially upon the temperature $-K = K_0 \exp(-Q/RT)$), as long as there is no temperature dependence of the time exponent, n.

Grain growth is usually studied by means of direct microscopic observations (optical and electron microscopy). In the case of extremely small grain size (nanocrystalline materials), accurate direct measure-

*Permanent address: Department of Chemistry, University of Sofia, 1126 Sofia, Bulgaria.

0022–2461

ments of the grain-size evolution are almost impossible. Chen and Spaepen [16] have shown that differential calorimetry can also be applied to determine the parameters that characterize the grain-growth process, especially in the case of large interface-to-volume ratio (if the grain size is less than about 10 nm).

The present work formed a quantitative microscopic (TEM) study of the processes of coarsening after complete crystallization of zirconium-based intertransition binary and ternary metallic glasses by measuring the grain size as a function of time and temperature. This paper presents practically the first results to be published on grain-growth kinetics in nanocrystalline materials. Additionally, information about the growth rates of nanocrystals in the amorphous matrix has been obtained for (Fe, Co)$_{33}$Zr$_{67}$ metallic glass.

2. Experimental procedure

Amorphous ribbons with compositions Fe$_{33}$Zr$_{67}$ and (Fe, Co)$_{33}$Zr$_{67}$ were prepared by melt-spinning on to a copper wheel (diameter 250 mm) in a helium atmosphere of 400 mbar.

X-ray (using CuK_α radiation) and electron diffraction studies were carried out on as-cast as well as on annealed ribbons to identify the amorphous state and to characterize the crystalline phases. The samples were heat-treated in a salt bath and at high temperatures because of the very fast crystallization by a technique for rapid heating. This technique uses electric current pulses with a well-controlled current intensity and time of the pulse through the sample [17]. During a typical rapid crystallization run, a piece of the ribbon (50 mm long) is resistively self-heated in a helium atmosphere from room temperature to a constant final temperature. During such a treatment the middle parts of the ribbons (about 6 mm) which were used for the TEM and X-ray analysis, do not exhibit any temperature gradient.

The calorimetric investigations were carried out using a Perkin–Elmer differential scanning microcalorimeter DSC-2C in an argon stream under isochronal conditions.

The microstructure at various stages during crystallization, as well as grain growth, were studied by TEM (Philips EM 301G) operating at 100 kV. Specimens were thinned by electrolytic jet polishing using an electrolyte of three parts methanol, one part glycerine and one part HNO_3, followed by ion-beam milling.

3. Results and discussion

3.1. (Fe, Co)$_{33}$Zr$_{67}$

X-ray and electron diffraction studies of the as-cast ribbons showed no trace of crystallinity. X-ray and electron diffraction patterns from the ribbons heat-treated over wide temperature range (below and above T_g) showed the presence of the stable tetragonal (Fe, Co)Zr$_2$ phase only (Fig. 1). Typical microstructure of the (Fe, Co)$_{33}$Zr$_{67}$ alloy heat treated for 20 s at 650 °C is shown in Fig. 1a. In contrast to the binary TM$_{33}$Zr$_{67}$ glasses, which first transform to a metastable nanocrystalline fcc phase and, after further annealing, into the stable tetragonal TMZr$_2$, the ternary (Fe, Co)$_{33}$Zr$_{67}$ glass crystallizes directly into the stable tetragonal (Fe, Co)Zr$_2$ phase. Except from TEM and electron diffraction studies, this is clearly seen from the DSC analysis carried out under scanning conditions (Fig. 2), as well as from the resistivity behaviour during the rapid heating experiments. In the case of (Fe, Co)Zr$_{67}$, only one exothermal peak, corresponding to the transformation of the amorphous material into the stable tetragonal phase has been observed, Fig. 2. To elucidate this different behaviour, further investigations on the crystallization mechanisms of the ternary zirconium-based intertransition glasses are necessary.

Grain growth was studied for the stable tetragonal (Fe, Co)Zr$_2$ phase, which crystallizes by a polymorphic reaction in the amorphous matrix. Mean grain

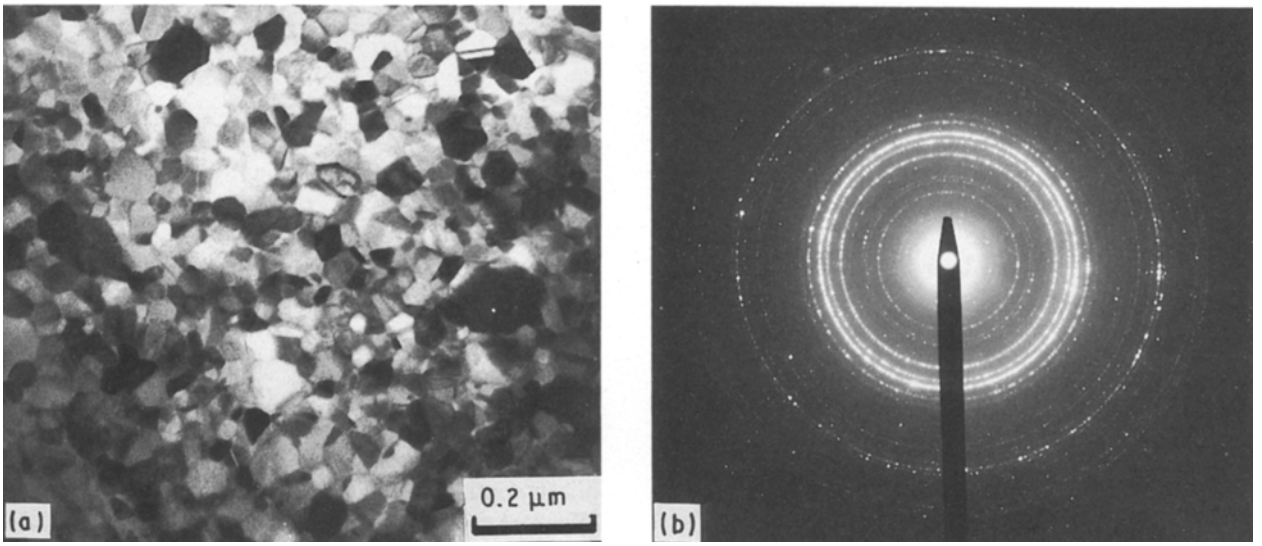

Figure 1 (a) Microstructure of (Fe,Co)$_{33}$Zr$_{67}$ melt-spun alloy annealed for 20 s at 650 °C, and (b) corresponding diffraction pattern of the tetragonal (Fe,Co)Zr$_2$ phase.

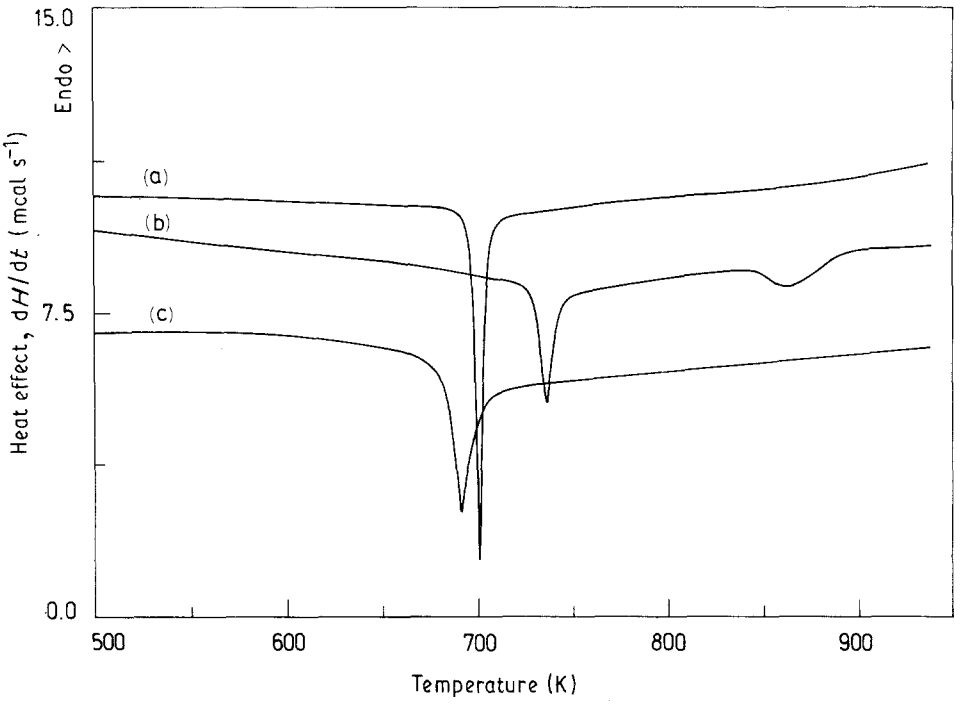

Figure 2 DSC thermograms of amorphous (a) $Fe_{16.5}Co_{16.5}Zr_{67}$, (b) $Co_{33}Zr_{67}$ and (c) $Fe_{33}Zr_{67}$, obtained at 40 K min^{-1} heating rate.

size (diameter, nm) determinations at various temperatures and times are presented in Table I. The average grain size, $\bar{D}$, obtained from the TEM image analysis was chosen as the representative value.

A plot showing the mean grain size as a function of time for three different constant temperatures is given in Fig. 3 in logarithmic coordinates. As can be seen from Fig. 3, in this case it is unreasonable to ignore the initial grain size, $\bar{D}_0$, in Equation 1. Only at large annealing times is the above dependence linear, i.e. $\bar{D}_0$ can be ignored. For this reason, the experimental data, $\bar{D} - t$, were fitted to the following equations

$$\bar{D} = 2ut \quad \text{for } t < t_{\text{cryst}} \quad (4)$$

$$\bar{D} = 2ut_{\text{cryst}} + c_{\text{gg}}(t - t_{\text{cryst}})^{1/n} \quad \text{for } t \geqslant t_{\text{cryst}} \quad (5)$$

where t_{cryst} is the time for complete crystallization, i.e. until the entire volume is composed of very small grains and the grains are in contact with one another, u is the growth rate of grains in the amorphous matrix, and c_{gg} is a constant dependent on certain physical parameters (including the mobility, grain-boundary free energy). The first term on the right-hand side of Equation 5 is connected to the crystal growth in the amorphous matrix with a constant growth rate, u; the second term, $c_{99}(t - t_{\text{cr}})^{1/n}$, is responsible for the second stage, i.e. the grain-growth after the amorphous matrix has been crystallized. $\bar{D}$, as a function of time, t, from the isothermal experiments (see Fig. 3) is best described by Equations 4, 5 with time exponent $n = 3$. The values of $n = 3$ are most frequently found in experimental works on grain-growth kinetics [18], despite the fact that grain-growth exponents of $n = 2$ are predicted from most grain-growth theories based on bulk diffusion. Unfortunately, the accuracy of the grain-size measurement for the small annealing times is insufficient, because of the small grain sizes (less than 5–8 nm). Therefore, direct calculation of u at small annealing times, according to Equation 4, was very difficult and inaccurate.

TABLE I Average grain size in crystallized $(Fe,Co)_{33}Zr_{67}$ ribbons at various temperatures and times

T (°C)	t (s)	Average grain size, D (nm)	Standard deviation S.D. (nm)
478	10	4.0	1.2
	25	7.5	1.8
	80	10.5	2.1
	1020	15.3	2.6
509	4	4.5	1.3
	10	8.0	2.1
	100	15.0	3.1
545	2	4.5	1.5
	4	6.5	1.9
	20	16.0	4.3
	100	23.0	5.2
	500	29.1	7.6
600	20	27.2	8.7
610	6	21.6	9.2
	20	29.8	8.9
650	5	30.9	9.2
	20	48.0	13.5
700	20	96.0	25.0
730	5	87.1	23.0
	20	136.2	26.0

At large annealing times, $t \gg t_{\text{cr}}$, we can neglect the first term in Equation 5 and it can then be written as

$$\bar{D} = c_{\text{gg}}(t - t_{\text{cryst}})^{1/3} \quad (6)$$

Equations 4 and 5 have been applied to describe the experimental $\bar{D} - t$ data for annealing times $t < t_{\text{cr}}$ and $t \geqslant t_{\text{cr}}$, respectively. The parameters in Equations 4 and 5, u, c_{gg} and t_{cryst} determined by fitting of the

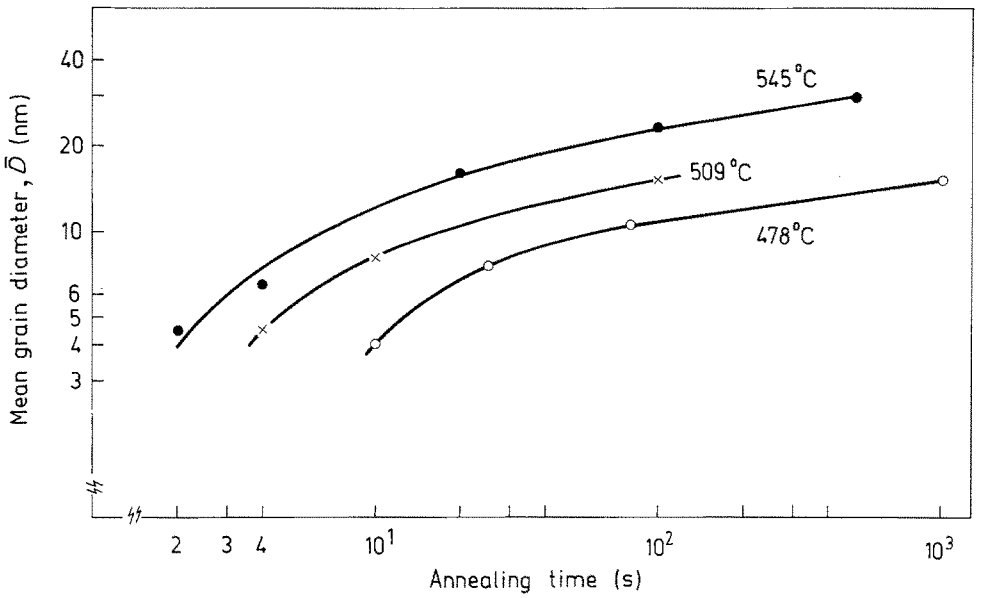

Figure 3 The mean grain size of $Fe_{16.5}Co_{16.5}Zr_{67}$ as a function of time for various annealing temperatures.

TABLE II Fitted parameters in Equations 4 and 5 for $(Fe,Co)_{33}Zr_{67}$

T (°C)	u (10^{10} ms^{-1})	c_{gg} (10^{10}ms$^{-1/3}$)	t_{cryst} (s)	S.D. (10^{10} m)
478	1.70 ± 0.03	9.26 ± 0.16	20.04 ± 0.32	5.17
509	4.12 ± 0.20	21.0 ± 0.94	6.98 ± 0.05	6.60
545	6.30 ± 0.08	22.4 ± 0.28	10.01 ± 0.19	10.2

experimental data to Equations 4 and 5, are presented in Table II. The evaluation of the above parameters (u, c_{gg} and t_{cryst}) has been carried out by non-linear regression (using Simplex and Newton numerical methods). In coordinates $\bar{D}$ versus t, smooth lines were drawn through the experimental data at each temperature. For the optimization procedure, approximately 15–20 points were taken from the $\bar{D}$–t curves, but to study the distribution of the differences between the experimental and calculated $\bar{D}$ values, only the experimental data were used. The standard deviation values (S.D.), which are a measure of the absolute error in the calculation of $\bar{D}$ (see Table II), were lower than the respective S.D. of the statistical determination of $\bar{D}$ at each temperature. This confirms the adequacy of the grain-growth model [4, 5] applied. It should be mentioned, however, that the differences between $\bar{D}_{exp}$ and $\bar{D}_{calc}$ according to Equations 4 and 5 were comparatively large at small annealing times but, nevertheless, they were lower than S.D. of the experimentally determined $\bar{D}$. The values of t_{cryst} and the corresponding $\bar{D}_0$ (calculated according to the expression $\bar{D}_0 = 2ut_{cryst}$) thus evaluated could be compared with the same parameters obtained from the direct TEM observations. This result showed that the fitting to the above grain-growth kinetic model (Equations 4 and 5) and in this way determination of the kinetic parameters is physically reliable.

The accuracy in the determination of the kinetic parameters in Equation 5 (including t_{cryst}) at $T = 509$ °C is lower compared with the other two temperatures (only three experimental $\bar{D}$–t points at $T = 509$ °C). Therefore, it is difficult to conclude from the t_{cryst} values that t_{cryst} goes through a minimum around 520 °C. Moreover, this is a very low temperature for the "nose" in the TTT diagram, compared with the other zirconium-based glasses [10].

The data from the isothermal experiments (three different temperatures) are not enough to obtain reliable values for the activation energies of crystal growth and grain growth from the temperature dependences of u and c_{gg}, respectively. The growth rates, u, found in this study are quite reasonable and comparable to the growth rates obtained in $Co_{33}Zr_{67}$ glass [17].

It was found that the grain-growth exponent, n, shows practically no temperature dependence, which differs from the observations of other investigators who obtained a strong temperature dependence of the time exponent [19].

Fig. 4 shows the experimental grain-growth results at different temperatures and times in coordinates $\lg(\bar{D}^n/t)$ versus $1/T$ according to Equations 3 or 6 using the value of $n = 3$ determined from the grain-growth isotherms (Fig. 3). All these experiments were carried out at large annealing times ($t \gg t_{cr}$), therefore the initial grain size, $\bar{D}_0$, was neglected in Fig. 4. The straight line suggests that the experimental data were consistent with the hypothesis that one mechanism was responsible for grain-growth over the whole temperature range studied (478–730 °C) and also supports the validity of the grain-growth mechanism ($n = 3$) as known for grain growth in various single-phase as well as two-phase systems [11, 18]. From the slope of

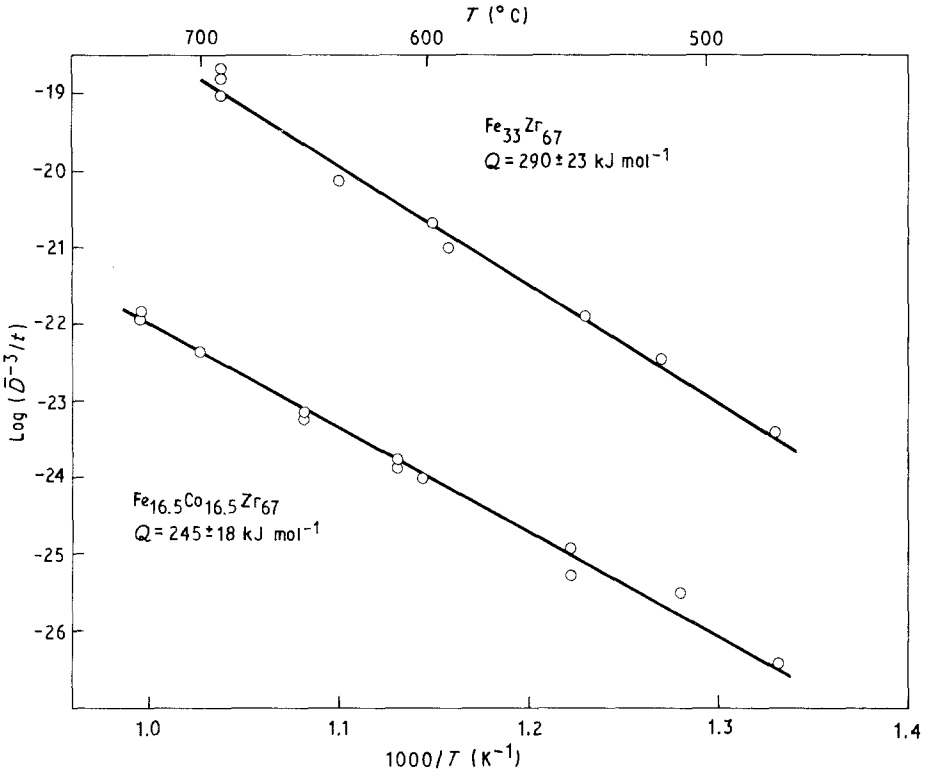

Figure 4 Temperature dependence of the grain-growth experimental data for $(Fe,Co)_{33}Zr_{67}$ and $Fe_{33}Zr_{67}$ according to Equation 3.

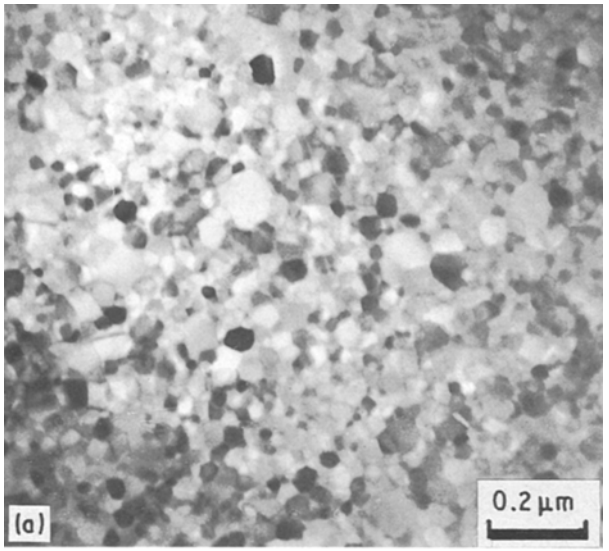

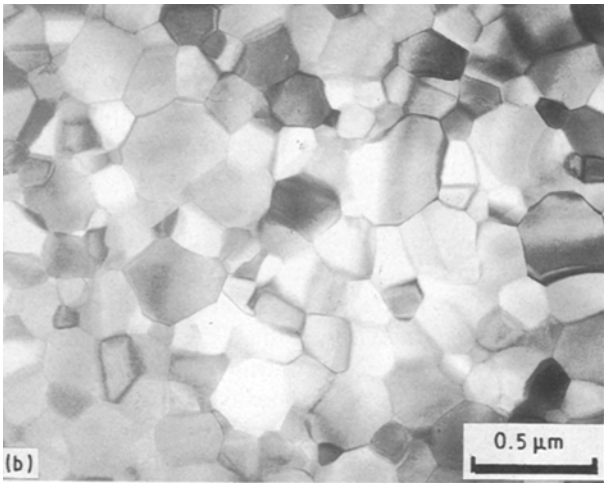

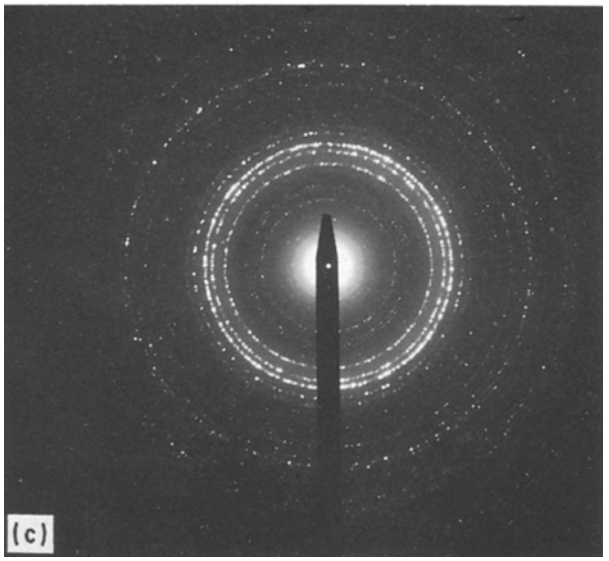

Figure 5 (a, b) Transmission electron micrographs and (c) corresponding diffraction pattern of the fcc $FeZr_2$ phase, after the first crystallization reaction during a rapid heating experiment; (a) 0.8 s, 540 °C and (b) 4.7 s, 595 °C.

the straight line in Fig. 4, the activation energy of the grain-growth process was determined to be $Q = 245 \pm 18\ kJ\ mol^{-1}$.

3.2. $Fe_{33}Zr_{67}$

Crystallization of various binary intertransition-metal glasses with 67 at % Zr ($TM_{33}Zr_{67}$, TM = Fe, Co, Ni) was studied. Above the glass transition temperature in all these glasses a very fast crystallization of a metastable fcc phase was observed thus leading to nanocrystalline microstructure. Among these glasses, only in $Fe_{33}Zr_{67}$ was a coarsening of the fcc metastable $FeZr_2$ phase observed before the transformation into

the stable tetragonal phase; this was studied quantitatively. It is well known from Altounian *et al.* [3], as well as from our TEM and resistivity studies of the crystallization behaviour of $Fe_{33}Zr_{67}$ glass, that crystallization occurs in two stages. Initially the amorphous ribbon crystallizes in the metastable fcc $FeZr_2$ phase (Fig. 5), which transforms (at about 1000 K) into the stable tetragonal $FeZr_2$ phase (Fig. 6).

According to Equation 3 the experimental grain-growth data for $Fe_{33}Zr_{67}$ are presented in Fig. 4. It is clearly seen that over a comparatively wide temperature range (480–690 °C), all the data lie on a straight line in the coordinates of Fig. 4, which once again confirms the validity of the grain-growth mechanism thus proposed for the case of the growth of nanocrystal grains in $(Fe,Co)_{33}Zr_{67}$ as well as in $Fe_{33}Zr_{67}$. The activation energy for grain-growth determined from the slope of the straight line in Fig. 4, $Q = 290 \pm 23\,kJ\,mol^{-1}$, is close to that obtained for growth of tetragonal $(Fe,Co)Zr_2$ crystal grains in $(Fe,Co)_{33}Zr_{67}$ alloy. This result also indicates that the same mechanism of grain-growth is valid for both glasses $Fe_{33}Zr_{67}$ and $(Fe,Co)_{33}Zr_{67}$. The results on grain growth of fcc $FeZr_2$ obtained by Yang [11] using *in situ* time-resolved X-ray diffraction, are very consistent with our grain-growth data. In the coordinates of Fig. 4, Yang's data [11] at 690 K lie practically on the same straight line (extrapolated at lower temperatures). Nevertheless, to find the mechanisms which control the grain-growth process, except for investigation of the grain-growth kinetics and activation energy, a study of the microstructure and some compositional parameters is necessary.

An interesting fact was that, despite approximately the same activation barriers, the absolute values of the kinetic constants, c_{gg}, in Equation 5 for the growth of the metastable fcc $FeZr_2$ crystals was about one order of magnitude larger than the corresponding values for the thermodynamically stable tetragonal $(Fe,Co)Zr_{67}$ crystals in practically the same temperature range. This was categorically confirmed from our TEM study of the coarsening of the stable tetragonal $FeZr_2$ crystals. The grain-growth velocities of the tetragonal $FeZr_2$ crystals were found to be much lower in comparison with those of fcc $FeZr_2$.

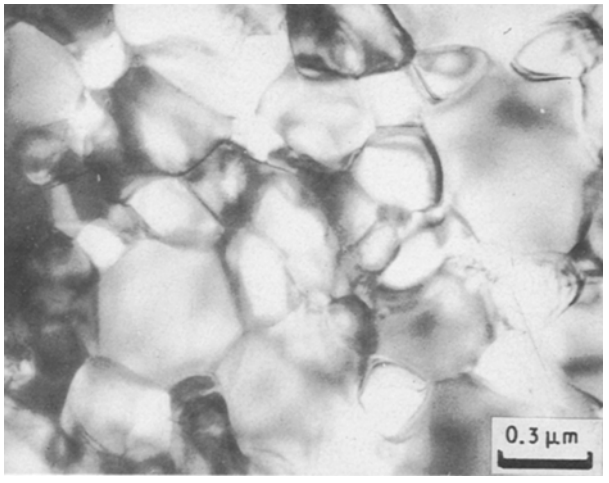

Figure 6 Microstructure of the stable tetragonal $FeZr_2$ phase.

4. Conclusions

The crystalline phase sequence during crystallization of the amorphous $Fe_{33}Zr_{67}$ and $(Fe,Co)_{33}Zr_{67}$ alloys was determined. Grain growth after crystallization of these glasses was observed. Crystallization and subsequent coarsening in the above alloys were studied quantitatively by TEM. It was found that for both systems, the grain-growth kinetics could be predicted by the model (Equation 5) with time exponent $n = 3$. This gives strong evidence that we indeed observed crystallization of a glass into a nanocrystalline material, rather than grain-growth in an extremely fine-grained material, which was never glassy at all, i.e. provides evidence of the amorphous structure of the as-cast material. Over a comparatively wide temperature range (about 200 °C) the grain-growth exponent, n, does not show a temperature dependence. The activation energies for grain-growth, about $260 \pm 25\,kJ\,mol^{-1}$, were found to be the same for both alloys. Using Equations 4 and 5, important information concerning the growth rates of the nanocrystals in the amorphous $(Fe,Co)_{33}Zr_{67}$ matrix was obtained.

Acknowledgement

This work was supported by the DFG (Ko 668/6).

References

1. K. H. J. BUSCHOW, *J. Less-Common Metals* **85** (1982) 221.
2. K. JANSSON and M. NYGREN, *Thermochim Acta* **114** (1987) 35.
3. Z. ALTOUNIAN, E. BATALLA, J. O. STROM-OLSEN and J. L. WALTER, *J. Appl. Phys.* **61**(1) (1987) 149.
4. Z. ALTOUNIAN, C. A. VOLKERT and J. O. STROM-OLSEN, *ibid.* **57** (1985) 1777.
5. W. SPRENGEL, W. DORNER and H. MEHRER, *Z. Metallkde* **81** (1990) 467.
6. Z. ALTOUNIAN, R. J. SHANK and J. O. STROM-OLSEN, *J. Appl. Phys.* **58** (1985) 1192.
7. D. S. EASTON, C. G. McKAMEY, D. M. KROEGER and O. B. CAVIN, *J. Mater. Sci.* **21** (1986) 1275.
8. K. JANSSON, M. NYGREN and A. OSTLUND, *Mater. Res. Bull.* **19** (1984) 1091.
9. H. R. SINNING, M. NICOLAUS and F. HAESSNER, in "Proceedings of the 7th Conference on RQM" edited by S. Savage and H. Frederiksson Stockholm (1990) p. 371.
10. U. KÖSTER and M. BLANK-BEWERSDORFF, *J. Less-Common Metals* **140** (1988) 7.
11. Y. YANG, PhD thesis, Montreal (1991).
12. H. V. ATKINSON, *Acta Metall.* **36** (1988) 469.
13. G. GREWAL, S. ANKEM, *ibid.* **38** (1990) 1607.
14. P. A. BECK, J. C. KREMER, L. J. DEMER and M. L. HOLZWORTH, *Trans. Amer. Inst. Min. Eng.* **175** (1948) 372.
15. J. E. BURKE and D. TURNBULL, *Prog. Metall. Phys.* **3** (1952) 220.
16. L. C. CHEN and F. SPAEPEN, *Mater. Sci. Engng* **A133** (1991) 342.
17. T. SPASSOV and U. KÖSTER, unpublished work.
18. M. P. ANDERSON, D. J. SROLOVITZ, G. S. GREST and P. S. SAHNI, *Acta Metall.* **32** (1984) 783.
19. R. L. FULLMAN, in ASM Seminar, "Metal Interfaces" (1987) p. 179.

Received 19 February
and accepted 29 October 1992